Experimental Neurology 311 (2019) 205–212

Contents lists available at ScienceDirect

Experimental Neurology

journal homepage: www.elsevier.com/locate/yexnr

Research Paper

Reduced Purkinje cell size is compatible with near normal morphology and function of the cerebellar cortex in a mouse model of spinocerebellar ataxia

Jakub Trzesniewski, Sandrine Altmann, Levy Jäger, Josef P. Kapfhammer*

Anatomical Institute, Department of Biomedicine Basel, University of Basel, Pestalozzistrasse 20, CH - 4056 Basel, Switzerland

ARTICLE INFO

Keywords:
Spinocerebellar ataxia type 14
Protein kinase C gamma
Purkinje cell dendritic development
Rapid Golgi staining
Climbing fiber innervation
pS6
C-Fos
Arc

ABSTRACT

Spinocerebellar ataxia type 14 (SCA14) is a dominantly inherited neurodegenerative disease caused by diverse mutations in the Protein Kinase C gamma (PKCγ) gene which is one of the crucial signaling molecules of Purkinje cells. We have previously created a mouse model of SCA14 by transgenic expression of a mutated PKCγ gene causing SCA14 with a mutation in the catalytic domain. Purkinje cells from the mutated mice have a strong reduction of their dendritic tree in organotypic slice cultures typical for increased PKC activity. There was no overt degeneration of Purkinje cells in vivo and the cerebellum appeared morphologically normal with the exception of lobule 7 where abnormal Purkinje cells were present. Besides from mild motor deficits the mice have no major phenotype. We have now done a more extensive study of cerebellar morphology in these mice and show by rapid Golgi staining that there is a marked reduction of Purkinje cell dendritic tree size throughout the cerebellum. Despite this reduction in dendritic tree size, climbing fiber innervation of Purkinje cells as visualized by immunostaining for the vesicular glutamate transporter 2 (vGlut2) appeared normal in most parts of the cerebellum. The same was true for the expression of the activity and plasticity markers pS6, c-Fos and Arc. These finding suggest that the cerebellar cortex in the transgenic mice is functioning fairly normal and that the reduction of dendritic tree size and the increased PKC activity can be compensated in most Purkinje cells. Around cerebellar lobule 7 there was high transgene expression from the L7 promotor and Purkinje cells showed abnormal morphologies. Climbing fiber innervation as well as the expression of the activity and plasticity markers was strongly disturbed in this area. Our results show that there is substantial potential for functional compensation in the cerebellar cortex. In lobule 7, an area with high transgene expression, compensation failed resulting in Purkinje cell degeneration and dysfunction.

1. Introduction

Spinocerebellar ataxias are mostly dominantly inherited neurodegenerative diseases which are characterized by cerebellar dysfunction and Purkinje cell degeneration, resulting in ataxia as a classic sign of cerebellar dysfunction (Soong and Paulson, 2007; Bushart et al., 2016). While some of the spinocerebellar ataxias are caused by extended glutamine repeats in the ataxin gene family (Paulson et al., 2017), a subgroup of spinocerebellar ataxias is caused by point mutations or small deletions in genes related to calcium signaling and homeostasis in Purkinje cells (Shimobayashi and Kapfhammer, 2018). In SCA14, mutations are present in Protein Kinase C gamma (PKCγ), the PKC isoform dominantly expressed in Purkinje cells. The mechanism by which the mutations induce Purkinje cell dysfunction and degeneration are not well understood. There is evidence for both gain-of-function and loss-of-function mechanisms contributing to SCA14 (Wong et al., 2018, Nakazone et al. 2018, Chopra et al., 2018) but the dominant inheritance would be compatible with a toxic gain-of-function mechanism (Pandolfo and van de Warrenburg, 2005). We have previously reported that in a transgenic mouse model of SCA14 with a mutation in the catalytic domain of PKCγ (S361G) we found evidence for Purkinje cell dysfunction, morphological abnormalities of Purkinje cells but no overt Purkinje cell degeneration (Ji et al., 2014). Interestingly, the dendritic tree of PKCγ-S361G transgenic Purkinje cells in organotypic slice cultures was severely reduced in size and resembled that of Purkinje cells exposed to stimulators of PKC (Metzger and Kapfhammer, 2000; Gugger et al., 2012) suggesting that this mutation confers increased biological activity of PKC (Shimobayashi and Kapfhammer, 2017) resulting in

Abbreviations: SCA14, Spinocerebellar ataxia type 14; PKCγ, protein kinase C gamma; vGlut2, vesicular glutamate transporter 2; pS6, phosphorylated form of ribosomal protein S6; GFP, green fluorescent protein; PB, 100 mM phosphate buffer; P18, postnatal day 18; CF territory, climbing fiber territory

* Corresponding author.
E-mail address: Josef.Kapfhammer@unibas.ch (J.P. Kapfhammer).

https://doi.org/10.1016/j.expneurol.2018.10.004
Received 1 June 2018; Received in revised form 27 September 2018; Accepted 9 October 2018
Available online 10 October 2018
0014-4886/

altered gene expression in PKCγ-S361G transgenic mice (Shimobayashi et al., 2016). Interestingly, the morphological changes of Purkinje cells were most pronounced in organotypic slice cultures from PKCγ-S361G transgenic mice but less evident in the cerebellum in vivo, where they were restricted to lobule 7 of the cerebellar cortex (Ji et al., 2014). We have now extended the morphological characterization of these mice by assessing Purkinje cell morphology by rapid Golgi staining. This method allows the morphological characterization of Purkinje cells throughout the cerebellum (van Hove et al., 2012). In addition, we studied climbing fiber innervation of Purkinje cell dendrites using vGlut2 immunohistochemistry (Hioki et al., 2003) and the expression of the neural activity and plasticity markers pS6 (Wullschleger et al., 2006), c-Fos (Sagar et al., 1988) and Arc (Steward and Worley, 2001; Kim and Thompson, 2011). Our results show that Purkinje cell dendritic morphology was compromised not only in lobule 7 of PKCγ-S361G transgenic mice but throughout the entire cerebellar cortex. In contrast, major abnormalities of climbing fiber innervation and expression of plasticity markers was restricted to the area of and around lobule 7 of the cerebellar cortex.

2. Materials and methods

2.1. Mice

Animal experiments were carried out in accordance with the EU Directive 2010/63/EU for animal experiments and were reviewed and permitted by Swiss authorities. Transgenic mice expressing PKCy carrying the S361G mutation (Ji et al., 2014) were used, and non-transgenic littermates or B6CF1 (CB6) mice were used as non-transgenic controls. The genotype of the transgenic mice was determined by PCR as previously described (Ji et al., 2014) and confirmed by observing GFP expression in Purkinje cells.

2.2. Golgi staining

A total of 39 mice (18 wild type and 21 S361G) were used for the Golgi study, ranging from ages P16 to age 15 months. The FD Rapid GolgiStain™ Kit (FD Neuro Technologies) was used for Golgi staining. Control and S361G transgenic mice were euthanized and briefly perfused with PBS. The cerebellum was dissected from the rest of the brain and collected in 4 ml of impregnation solution according to the manufacturer's instructions. After 2–3 weeks of incubation, the cerebella were placed in solution C from the kit and stored at 4 °C for 3 to 4 days. Then, the cerebella were frozen in isopentane at approximately −80 °C without embedding. Once frozen, the brains were kept at −80 °C for 5 to 10 min before being stored at −20 °C. Sections were cut at 100 μm using a Leica CM1900 cryostat, collected and mounted on gelatin coated-slides using solution C and dried overnight in the dark. The next day, the staining was developed using solutions D, E and distilled water at a 1:1:2 concentrations. The sections were then dehydrated in increasing alcohol concentrations and coverslipped using Eukitt mounting medium (Sigma-Aldrich, Switzerland). Slides were viewed on a Zeiss Axioscope microscope and images were taken using a Zeiss AxioCam imaging system (Zeiss, Germany).

2.3. Immunohistochemistry

A total of 32 mice were used for the immunohistochemical study (16 wild type and 16 S361G mice). For each developmental time point at least two mice per genotype were analyzed. Mice were perfused with 4% paraformaldehyde and the cerebellum was dissected. After cryoprotection in 30% sucrose for 24 h the cerebellum was covered with Tissue-Tek (Sakura), frozen in −40 °C cold isopentane and stored at −20° until further use. Frozen sections were cut on Leica CM1900 cryostat at 25 μm. Sections were incubated free floating with the following antibodies: rabbit anti-calbindin D28K and mouse monoclonal anti-Calbindin (1:1000, Swant, Marly, Switzerland), guinea pig anti vGlut2 (1:1000, Merck Millipore, Germany), rabbit anti-PKCγ (1:1000, Santa Cruz Biotechnology, Santa Cruz, CA), rabbit anti-GFP (1:500, Novus, Zug, Switzerland), rabbit anti-Phospho-S6, (1:500, Cell Signaling, USA), rabbit anti-cFos (1:500, Merck-Millipore, Germany), rabbit anti-Arc (1:500, Synaptic Systems, Germany).

All reagents were diluted in 100 mM phosphate buffer (PB), pH 7.3. Primary antibodies were added in fresh blocking solution (0.1–0.3% Triton X-100, 3% normal goat serum) and incubated overnight at 4 °C. The staining was visualized with anti-mouse and anti-rabbit AlexaFluor 488 and 568 2nd antibodies or anti-guinea pig AlexaFluor 568 (1:500, Molecular Probes, Eugene, OR). After washing in PB, secondary antibodies were added in PB containing 0.1% Triton X-100 in order to prevent non-specific antigen binding for at least 1 h at room temperature. Stained sections were mounted on Superfrost glass slides (Menzel, Braunschweig, Germany) and coverslipped with Mowiol (Sigma Aldrich, Buchs, Switzerland). Sections were viewed on an Olympus AX-70 microscope equipped with a Spot digital camera. Recorded images were adjusted for brightness and contrast with Photoshop image processing software.

2.4. Statistical analysis

The quantification of Purkinje cell dendritic tree size was done as previously described (Sherkhane and Kapfhammer, 2017). An image analysis program (ImageJ) was used to trace the outline of the Purkinje cell dendritic trees yielding the area covered by the dendritic tree and the length of the longest dendrite. The analysis was performed in adult mouse brains age 7–9 months. A total of 15–30 Purkinje cells were acquired from one cerebellum, representing all or the majority of all Golgi-stained Purkinje cells per cerebellum. The measurements from three different brains were pooled and statistical differences were analyzed using GraphPad Prism software (San Diego, USA). The mean value of the wild type mice was set as 100%. Data are shown as the mean ± S.D. The statistical significance of differences in parameters was assessed by non-parametric Mann-Whitney's test. Confidence intervals were 95%, statistical significance when $p < .05$.

The CF territory was determined by measuring the expansion of climbing fibers into the molecular layer on cerebellar sections. Measurements were made using ImageJ on a minimum of 4 different sections per condition. The thickness of the molecular layer was measured as the distance from the Purkinje cell layer to the pial margin of the molecular layer, and the climbing fiber extension by measuring the distance from the Purkinje cell layer to the end of climbing fiber innervation in the molecular layer. The CF territory value was calculated by diving the climbing fiber extension by the molecular layer thickness for each measurement. Statistical analysis was done using GraphPad Prism software (San Diego, USA). The statistical significance of differences in the parameters was assessed by non-parametric analysis of variance (Kruskal-Wallis test) followed by Dunn's post test.

CF puncta were counted on vGlut2-stained sections using ImageJ. The number of immunopositive puncta was counted in a square of defined size at three locations of the molecular layer of cerebellar lobules located either in the anterior lobe or in lobule 7. Measurements were made on a minimum of 4 different sections per condition. Statistical analysis was done using GraphPad Prism software (San Diego, USA). The statistical significance of differences in the parameters was assessed by non-parametric analysis of variance (Kruskal-Wallis test) followed by Dunn's post test.

3. Results

3.1. Purkinje cells in S361G-PKCγ transgenic mice have abnormal dendritic trees with reduced size

We have previously shown that the cerebellum of S361 transgenic mice has an essentially normal morphology, and most Purkinje cells

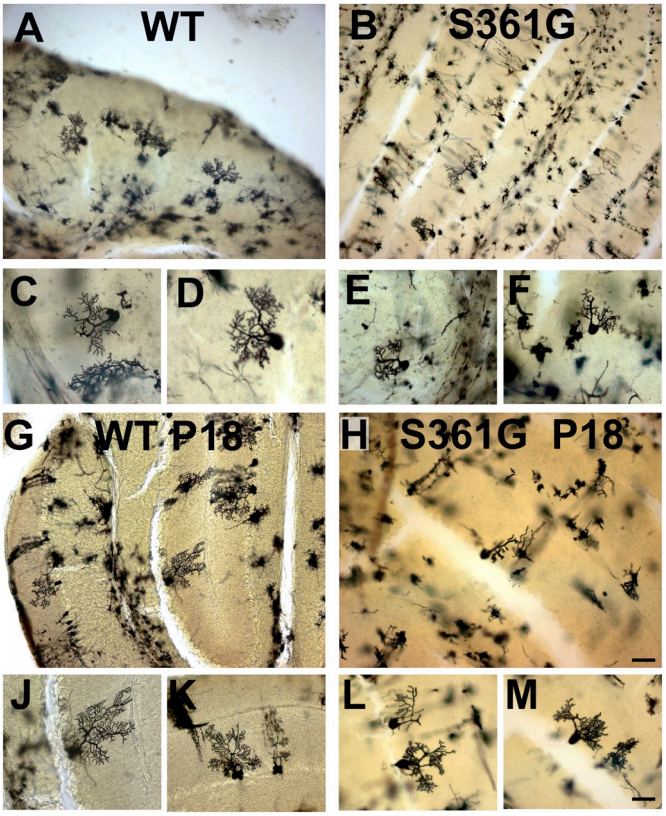

Fig. 1. Golgi staining of Purkinje cells.
A, B Low power images (10×) of Golgi stainings of the cerebellum of 15 months old wild type mice (A) and S361G-PKCγ transgenic mice (B). Purkinje cells in S361G-PKCγ transgenic mice did not cover the entire width of the molecular layer. C - F At higher magnification (20×) Purkinje cells with well differentiated dendritic trees can be seen in wild type mice (C, D). Purkinje cells in S361G-PKCγ transgenic had smaller, more condensed dendritic trees (E, F). G, H Low power view (10×) of the cerebellum from P18 mice. There are several Purkinje cells with well extended dendritic trees visible in wild type mice (G), Purkinje cells in S361G-PKCγ transgenic mice had smaller less branched dendritic trees (1H). J – M At higher power (20×), Purkinje cells with large dendritic trees were present in wild type mice (I,K). Purkinje cells from S361G-PKCγ transgenic mice were smaller and the dendritic braches appeared more condensed (L, M). Scale bar in H for A, B, G, H = 100 μm, in M for C, D, E, F, I, K. L, M = 50 μm.

appear to have a normal dendritic tree based on immunohistochemical anti-Calbindin staining (Ji et al., 2014). We have now used a rapid Golgi stain in order to visualize the dendritic tree of Purkinje cells of control and transgenic mice. It is evident already from low power views (10× lens) that Purkinje cells in adult S361G-PKCγ transgenic mice (15 months old) had smaller dendritic trees compared to control mice (Fig. 1A and B). When viewed at higher magnification, Purkinje cells from control mice had Purkinje cells with the typical large dendritic trees (Fig. 1C, D). In contrast, Purkinje cells from S361G-PKCγ mice had smaller, more condensed dendritic trees (Fig. 1E, F). This difference was present throughout all parts of the cerebellum. In the lower part of the figure, images from P18 mice are shown, a time point immediately after rapid extension of the Purkinje cell dendritic trees (Armengol and Sotelo, 1991; Kapfhammer, 2004). In the wild type cerebellum, Purkinje cells have well developed dendritic trees spanning the whole width of the molecular layer (Fig. 1G). At higher magnification the branching pattern with many higher order branches is evident (Fig. 1J, K). In contrast, Purkinje cells in S361G-PKCγ mice had smaller dendritic trees with less side branches (Fig. 1H). At higher magnification, side branches appear to be condensed and have a reduced number of higher order branches (Fig. 1L, M). We quantified the dendritic trees of Purkinje cells in adult (7–9 months old) control and

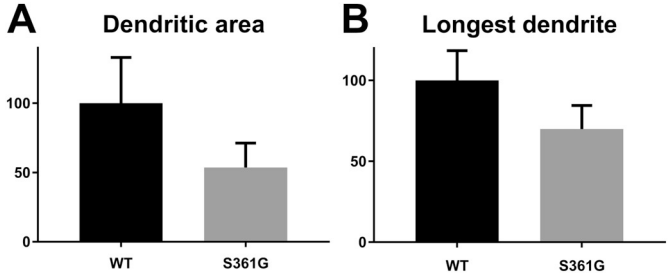

Fig. 2. Quantification of Purkinje cell dendritic tree size.
The area covered by the dendritic tree and the length of the longest dendrite were measured in Purkinje cells from adult (7–9 months) old mice. All Purkinje cells present in the Golgi-stainings on sections from the vermis and the adjacent part of the hemispheres were measured. The n was 52 for WT and of 94 for the S361G-PKCγ mice.The mean value of the wild type mice was set as 100%. Data are shown as the mean ± S.D. A The area covered by Purkinje cells in S361G transgenic mice was reduced to 54% of that of wild type mice. B The length of the longest dendrite in S361G transgenic mice was reduced to 70% of that of wild type mice. Both results were significant with $p < .0001$ in the Mann-Whitney test.

S361G-PKCγ transgenic mice. While the rapid Golgi method stains many cells in the cerebellar cortex the number of visualized Purkinje cells was rather limited (see for example Fig. 1B). For the quantification, we used all sections from a particular cerebellum which included sections of the vermis and the adjacent medial part of the hemispheres (but not the lateral part of the hemispheres). All Golgi-stained Purkinje cells present in the sample were analyzed and this yielded only 15–40 Purkinje cells per cerebellum. From the three cerebella which were analyzed for each genotype, we got an "n" of 52 for WT cerebellum and of 94 for the S361G-PKCγ cerebellum. The mean value of the wild type mice was set as 100%. Data are shown as the mean ± S.D. The mean for the dendritic area was reduced to 54% of the control value for Purkinje cells from S361G-PKCγ transgenic mice (Fig. 2A). The reduction was less strong for the length of the longest dendrite which was reduced to 70% (Fig. 2B). Both differences were significant with $p < .0001$. A similar reduction of dendritic tree size was also found for mice at other ages including P16-P19 mice, the earliest age studied (quantitative data not shown, but see Fig. 1G-1M). The Golgi staining showed that despite the rather normal appearance of Purkinje cells in Calbindin immunohistochemistry there was a widespread reduction of Purkinje cell dendritic tree size in S361G-PKCγ transgenic Purkinje cells throughout the cerebellum.

3.2. Normal climbing fiber innervation of Purkinje cells in most parts of the cerebellum of S361G-PKCγ transgenic mice

We analyzed climbing fiber innervation in adult, 3 months old mice by immunohistochemistry with an anti-vGlut2 antibody. In the cerebellar molecular layer, vGlut2 is specifically expressed only in climbing fibers (Hioki et al., 2003). The antibody staining revealed an innervation of Purkinje cell dendrites in the inner 80% of the molecular layer in control animals (Fig. 3B). Because the transgene is expressed from a plasmid together with GFP, Purkinje cells in S361G-PKCγ transgenic mice, but not Purkinje cell in control mice, express GFP. In the wild type control, no anti-GFP staining was present (Fig. 3A). In contrast, in S361G-PKCγ transgenic mice, GFP expression was present and revealed Purkinje cells and their dendritic trees (Fig. 3D). In most parts of the cerebellum of S361G-PKCγ transgenic mice, vGlut2 staining was similar as in control mice. It covered the inner 80% of the molecular layer leaving the outermost part free (Fig. 3B and E, quantification shown in Fig. 3N).

3.3. Maturation of climbing fiber innervation is similar in wild type and S361G-PKCγ transgenic mice

We have studied the development and maturation of climbing fiber innervation in S361G-PKCγ transgenic mice. Before P14, climbing

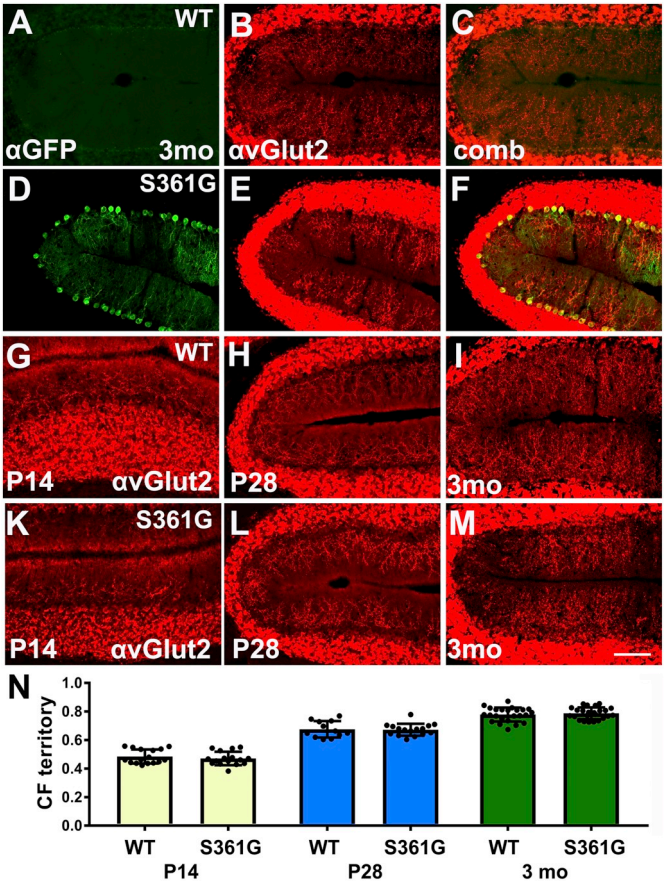

Fig. 3. Climbing fiber innervation of the wild type and S361G cerebellum.
A - C Immunostaining for the climbing fiber marker vGlut2 in wild type cerebellum. A Transgenic expression of GFP is absent in wild type cerebellum. B Anti-vGlut2 immunostaining reveals the climbing fiber innervation of the inner 80% of the molecular layer. C Because anti-GFP staining was absent, the double-staining is mostly identical to the vGlut2 staining.
D – F Immunostaining for anti-vGlut2 in the S361G cerebellum. D Anti-GFP immunostaining shows Purkinje cells with varying intensity of transgene expression. E Anti-vGlut2 staining reveals the climbing fiber innervation also covering approximately 80% of the molecular layer similar as in wild type cerebellum. F The double staining shows normal climbing fiber innervation in the molecular layer with transgenic Purkinje cell dendritic trees.
G - I Postnatal progression of climbing fiber innervation in the wild type cerebellum. G Immunostaining for the climbing fiber marker vGlut2 in the P14 WT cerebellum covers approx. 50% of the molecular layer thickness. H At P28, climbing fibers cover approx. 70% of the molecular layer thickness. I At 3 months, climbing fibers cover approx. 80% of the molecular layer thickness.
K – M Postnatal progression of climbing fiber innervation in the S361G cerebellum. K In the P14 S361G cerebellum climbing fibers also cover approx. 50% of the molecular layer thickness. L At P28, climbing fibers also cover approx. 70% of the molecular layer thickness in the S361G cerebellum. M At 3 months, climbing fibers cover approx. 80% of the molecular layer thickness in the S361G cerebellum. Scale bar in M for A - M = 100 μm.
N Quantification of the climbing fiber territory for wild type and S361G mice at P14, P28 and 3 months. The CF territory increased from approx. 48% at P14 to 68% at P28 and reached 79% at 3 months. No major differences were observed between wild type and S361G mice.

fibers cannot be unequivocally identified by vGlut2 immunostaining because also parallel fiber terminals at these stages express vGlut2 (Miyazaki et al., 2003). At P14, in most parts of the cerebellum there was a still rather sparse innervation of the Purkinje cell dendrites by climbing fibers. At this stage, climbing fibers were more abundant in the inner half of the molecular layer and only occasionally spread into the distal half of the molecular layer (Fig. 3G and K). On average, they covered < 50% of the molecular layer (Fig. 3N). The pattern was similar in wild type (Fig. 3G) and in S361G-PKCγ transgenic mice (Fig. 3K) and in both genotypes a similar fraction of the molecular layer was covered by climbing fibers (Fig. 3N). At 4 weeks of age, climbing fiber innervation had increased in density and extended to about 70% of the molecular layer thickness. This was true both for the wild type (Fig. 3H) and the S361G-PKCγ transgenic mice (Fig. 3L, quantification in 3 N). In both wild type (Fig. 3I) and S361G-transgenic mice (Fig. 3M) climbing fiber innervation covered approximately 80% of the molecular layer in 3 months old mice. We have quantified the climbing fiber territory (i.e. the extension of climbing fibers towards the outer margin of the molecular layer) in wild type and S361G mice on sections from the vermis. The climbing fiber territory increased from 48% in P14 mice to 68% in P28 and to 79% in 3 months old mice. No major differences between wild type and S361G mice were observed (Fig. 3N).

3.4. Reduced climbing fiber innervation in lobule 7 of S361G-PKCγ transgenic mice

We have previously reported that in lobule 7 of the cerebellar vermis the phenotype of the S361G-PKCγ transgenic mice is more prevalent and Purkinje cells have an abnormal morphology with greatly reduced and condensed dendritic trees (Ji et al., 2014). This was also reflected in the climbing fiber innervation. In wild type mice at P28 there were climbing fibers present throughout the molecular layer of lobule 7 (Fig. 4A–C). In S361G-PKCγ transgenic mice, the Purkinje cell layer was disorganized and Purkinje cells which strongly expressed GFP and which had abnormal dendritic trees were present (Fig. 4D, G). In these areas, the density of climbing fiber innervation was greatly reduced (Fig. 4E, H). At higher magnification, it is obvious that climbing fibers were only present at the cell soma and the initial parts of the dendrites very close to the soma. The more distal parts of the dendritic tree remained free of climbing fibers (Fig. 4H). The tight association of climbing fibers with the soma and the initial part of the dendritic tree is particularly obvious in the double staining (Fig. 4J). In these cells, the transition of climbing fiber innervation from the soma to the more distal dendrites is impaired. Some Purkinje cells in lobule 7 were almost completely devoid of climbing fiber innervation (arrowheads in Fig. 4H and J).

At the age of three months, there was still a similar overall depletion of climbing fiber innervation in lobule 7 (Fig. 4K–M). Some Purkinje cells still had a sparse climbing fiber innervation in the more distal part of their dendritic tree (Fig. 4K–M, cells on the left) whereas other cells had lost climbing fiber innervation almost completely (Fig. 4K–M, cell shown by white arrow). In other cells, climbing fiber innervation was restricted to the cell soma and the primary dendrites as described above (Fig. 4K–M, cell shown by white arrowhead and cell at bottom right) indicating that the transition from innervation of the soma to the more distal dendrites was impaired in these Purkinje cells. These findings suggest that Purkinje cells with a dystopic location and strong expression of the S361G-PKCγ transgene have an abnormal and reduced climbing fiber innervation.

We have quantified the density of climbing fiber innervation by counting vGlut2-positive puncta in the molecular layer of 4 week old mice. In lobules of the anterior lobe, no difference was found between wild type and S361G mice (Fig. 4N, left). In contrast, in lobule 7, there was a strong reduction of climbing fiber innervation to < 50% of the wild type values (Fig. 4N, right). This difference was statistically significant with $p < .001$.

3.5. Suppression of PI3K/Akt/mTORC1 signaling in lobule 7 in Purkinje cells with dystopic location and highly abnormal dendritic trees

The activity of the PI3K/Akt/mTORC1 signaling pathway can be monitored by the phosphorylation of the ribosomal protein S6 (Wullschleger et al., 2006). This fundamental signaling pathway is essential for many cell functions and developmental processes. In the

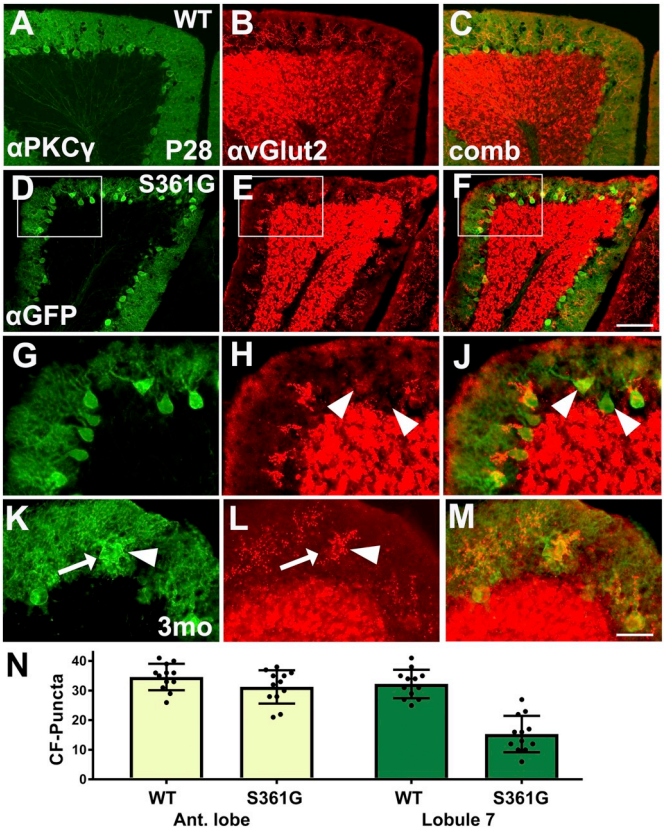

Fig. 4. Impaired climbing fiber innervation around lobule 7 of the cerebellar cortex of S361G-PKCγ transgenic mice.

A - C Immunostaining of cerebellar lobule 7 for the climbing fiber marker vGlut2 in P28 wild type cerebellum. A Purkinje cells are labelled with anti-PKCγ. B Anti-vGlut2 immunostaining reveals climbing fiber innervation extending to about 70% of the molecular layer thickness. C Double-staining for PKCγ and vGlut2.

D - F Immunostaining of cerebellar lobule 7 for the climbing fiber marker vGlut2 in P28 S361G cerebellum. D Several Purkinje have strong transgene expression as revealed by GFP expression, some have a dystopic location in the molecular layer. E Anti-vGlut2 immunostaining shows only very scarce climbing fiber innervation restricted to the Purkinje cell soma and proximal dendrites. F Double-staining for PKCγ and vGlut2.

G - J The boxed areas from D - F are shown at higher magnification in G – J. In H and J, it is obvious that the climbing fibers only cover the soma and proximal dendrites of Purkinje cells but do not spread to the outer parts of the molecular layer. Arrowheads in H and J label two Purkinje cells virtually devoid of climbing fiber innervation.

K - M Immunostaining of cerebellar lobule 7 for the climbing fiber marker vGlut2 in 3 months old S361G cerebellum (higher magnification). K Two Purkinje cells are strongly GFP-positive and are labelled by an arrow and an arrowhead. L Anti-vGlut2 immunostaining shows that the left Purkinje cell (white arrow) is almost completely devoid of climbing fiber innervation while the right cell (arrowhead) receives climbing fiber innervation restricted to the cell soma and the primary dendrites. M Double-staining for PKCγ and vGlut2. Scale bar in F for A – F = 100 μm, in M for G - M = 50 μm.

N Quantification of vGlut2-positive puncta representing climbing fiber innervation in the molecular layer (CF puncta) of P28 mice. In lobules of the anterior lobe, there was no major difference in the number of CF puncta between wild type and S361G mice. In contrast, innervation densitiy was reduced to 48% of control values in lobule 7. This difference was statistically significant with $p < .01$.

cerebellum of wild type mice, Purkinje cells are positive for pS6 to a varying degree, and the intensity of the staining may reflect different activation states of this pathway in different cells (Fig. 5A–C, G–K). In most parts of the cerebellum from S361G-PKCγ transgenic mice, pS6

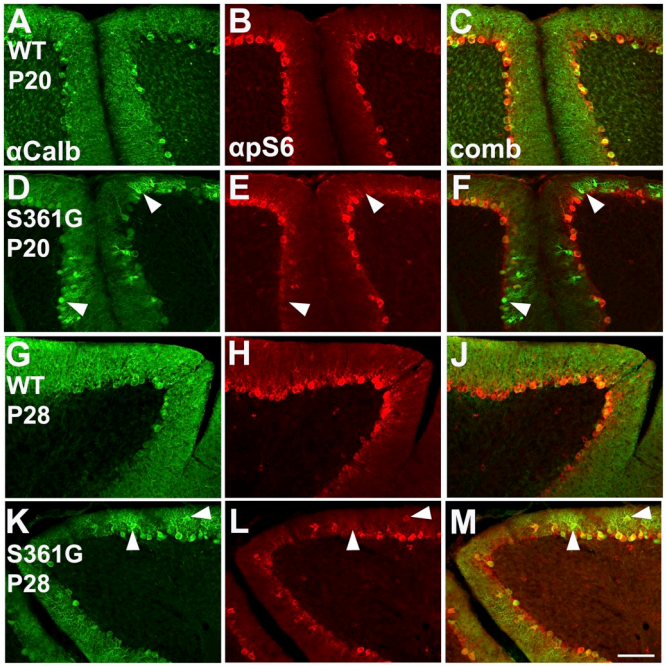

Fig. 5. Suppression of staining for the phosphorylated protein S6 (pS6) in Purkinje cells around lobule 7 of the cerebellar cortex of S361G-PKCγ transgenic mice.

A - C Immunostaining of the transition between cerebellar lobules 6 and 7 for pS6 in 3 week old (P20) wild type mice. A Purkinje cells are labelled with anti-Calbindin. B Anti-pS6 immunostaining was present in all Purkinje cell somata in wild type mice. C Double-staining for Calbindin and pS6 confirms the presence of pS6 in all Purkinje cells.

D - F Immunostaining of the transition between cerebellar lobules 6 and 7 for pS6 in 3 week old (P20) S361G-PKCγ transgenic mice. D Calbindin staining reveals several Purkinje cells with abnormal morphology and dystopic location. Two such cells are labelled with arrowheads. E Most Purkinje cells located in the Purkinje cell layer express pS6. In contrast, Purkinje cells with abnormal dendrites and dystopic location were often pS6 negative. F Double staining confirms absence of pS6 staining in dystopic and abnormal Purkinje cells.

G - J Immunostaining of cerebellar lobule 7 for pS6 in 4 week old (P28) wild type mice. G Purkinje cells are labelled with anti-Calbindin. H Anti-pS6 immunostaining was present in all Purkinje cell somata in wild type mice. J Double-staining for Calbindin and pS6 confirms the presence of pC6 in all Purkinje cells.

K - M Immunostaining of cerebellar lobule 7 for pS6 in 4 week old (P28) S361G-PKCγ transgenic mice. K Calbindin staining reveals several Purkinje cells with abnormal morphology and dystopic location. Two such cells are labelled with arrowheads. L Most Purkinje cells located in the Purkinje cell layer express pS6. In contrast, Purkinje cells with abnormal dendrites and dystopic location were often pS6 negative. M Double staining confirms absence of pS6 staining in dystopic and abnormal Purkinje cells. Scale bar in M for A - M = 100 μm

expression is similar to that in wild type cerebellum (data not shown). In contrast, Purkinje cells with a dystopic location in the molecular layer and a highly abnormal dendritic tree at the transition from lobule 6 to lobule 7 (arrowheads in Fig. 5D–F) were negative for pS6, indicating a suppression of the PI3K/Akt/mTORC1 signaling pathway. A cerebellar lobule 7 from 4 week old mice is shown in Fig. 5G–M. In the wild type mouse, all Purkinje cells in lobule 7 were positively stained for pS6 (Fig. 5G–J). In the S361G-PKCγ mouse, several Purkinje cells located correctly in the Purkinje cell layer showed a normal pS6 staining. In contrast, some Purkinje cells which had a dystopic location in the molecular layer and had abnormal dendritic trees indicative of Purkinje cell dysfunction did not express pS6 (Fig. 5K–M, dystopic cells indicated by arrowheads). Our data indicate that the PI3K/Akt/mTORC1 signaling pathway is suppressed in dystopic Purkinje cells of lobule 6 and 7 suggesting that these cells are dysfunctional.

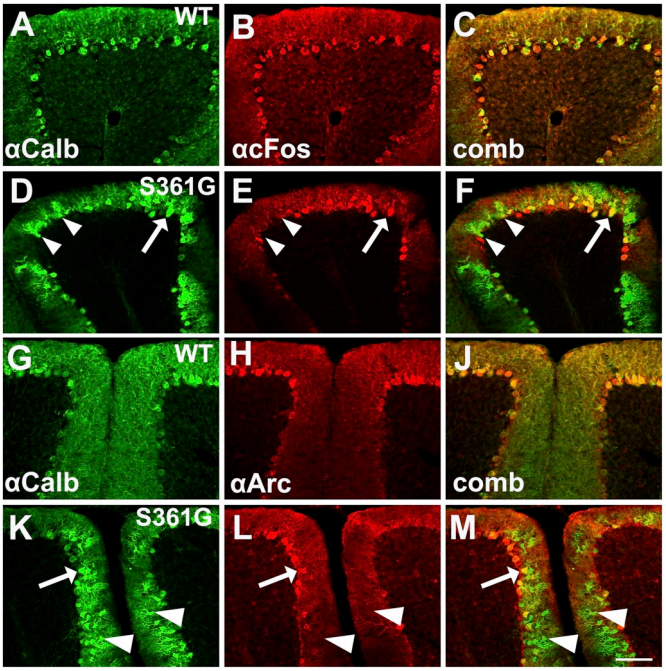

Fig. 6. Suppression of c-Fos and Arc in Purkinje cells in lobule 7 of the cerebellar cortex of S361G-PKCγ transgenic mice.
A - C Immunostaining of cerebellar lobule 7 for c-Fos in P20 wild type mice. A Purkinje cells are labelled with anti-Calbindin. B Anti-c-Fos immunostaining was present in all Purkinje cell somata in wild type mice. C Double-staining for Calbindin and c-Fos confirms the presence of c-Fos in all Purkinje cells.
D - F Immunostaining of cerebellar lobule 7 for c-Fos in P20 S361G-PKCγ transgenic mice. D Calbindin staining reveals several Purkinje cells with abnormal morphology and dystopic location. Two such cells are labelled with arrowheads, one with an arrow. E Purkinje cells with abnormal dendrites and dystopic location were often c-Fos negative (arrowheads). Some abnormal Purkinje cells were also strongly c-Fos positive (arrow). F Double staining confirms the absence of c-Fos staining in many dystopic and abnormal Purkinje cells (arrowheads). Some of these cells also were c-Fos positive (yellow cells in the right part of the lobule, arrow).
G - J Immunostaining of the transition between cerebellar lobules 6 and 7 for Arc in 3 week old (P20) wild type mice. G Purkinje cells are labelled with anti-Calbindin. H Anti-Arc immunostaining was present in all Purkinje cell somata in wild type mice. C Double-staining for Calbindin and pS6 confirms the presence of pC6 in all Purkinje cells.
K - M Immunostaining of cerebellar lobule 7 for pS6 in 4 week old (P28) S361G-PKCγ transgenic mice. K Calbindin staining reveals several Purkinje cells with abnormal morphology and dystopic location. Two such cells are labelled with arrowheads, one with an arrow. L Purkinje cells with abnormal dendrites and dystopic location were often Arc negative (arrowheads) but a few were also Arc positive (arrow). F Double staining confirms absence of Arc staining in most dystopic and abnormal Purkinje cells. Scale bar in M for A - M = 100 μm

3.6. Suppression of the activity and plasticity markers c-Fos and Arc in lobule 7 in Purkinje cells with dystopic location and highly abnormal dendritic trees

The immediate early gene c-Fos has been shown to be expressed with neural activity (Sagar et al., 1988) and is now widely used as a marker for neural activation. We have used c-Fos to see whether the Purkinje cells in S361G-PKCγ transgenic mice have altered levels of activity. In 3-week old control mice, c-Fos was expressed to varying degrees in most Purkinje cells of the cerebellar cortex (Fig. 6A–C). A similar widespread expression of c-Fos was found in the Purkinje cells of S361G-PKCγ transgenic mice. However, in lobule 7 where Purkinje cells with a dystopic location in the molecular layer and altered dendritic morphology are common, c-Fos immunoreactivity was typically absent from these abnormal cells (Fig. 6D–F, two c-Fos negative cells are labelled with arrowheads). However, a few abnormal cells were strongly positive for cFos (white arrow in Fig. 6D–F) indicative of a strong activation of these cells.

The cytoskeletal protein Arc is also considered to be a marker for neuronal activity and plasticity. It was shown to be selectively targeted to active synapses (Steward and Worley, 2001). In the cerebellum of 3-week old wild type mice we found again a solid expression of Arc in the majority of Purkinje cells (Fig. 6G–J). This was similar in most parts of the cerebellum from S361G-PKCγ transgenic mice. When we looked at the border between lobule 6 and 7 we found again many Purkinje cells with altered dendritic trees and a dystopic location in the molecular layer. Most of these cells were negative for Arc immunoreactivity (arrowheads in Fig. 6K–M) suggesting that they only had a low activity level. Similar as for c-Fos, a few dystopic cells with altered morphology were also positive for Arc (arrow in Fig. 6K–M).

The findings from the two immediate early genes, c-Fos and Arc, are very similar. While in most parts of the S361G-PKCγ transgenic cerebellum the expression of these markers was comparable to wild type mice, the Purkinje cells in lobule 7 with dystopic location and altered dendritic morphology were mostly negative for these immediate early genes.

4. Discussion

In this study we have extended the morphological analysis of changes in the cerebellum of the S361G-PKCγ mouse, a mouse model of SCA14. Using rapid Golgi staining we show that there is a marked size reduction of the Purkinje cell dendritic tree in this mouse throughout the cerebellar cortex. In contrast, climbing fiber innervation as studied by vGlut2 immunoreactivity appeared to be normal in most parts of the cerebellum but was strongly disturbed in lobule 7 where the morphological changes of Purkinje cells are most prominent. The same applied for immunostaining with the activity and plasticity markers pS6, c-Fos and Arc which all showed a rather normal pattern in most parts of the cerebellum, but were greatly altered in lobule 7. Our results show that the general reduction of Purkinje cell dendritic tree size in the S361G-PKCγ mouse can be compensated in most parts of the cerebellum and is compatible with a normal development of climbing fiber innervation and normal expression of global activity markers. In contrast, in lobule 7, an area with high transgene expression and with abnormal Purkinje cells, all these parameters are disturbed and the cerebellar cortex here appears to be dysfunctional. Our findings show that the cerebellar cortex can compensate a certain increase of PKC activity and a reduction of Purkinje cell dendritic tree size but becomes dysfunctional with very high PKC activity leading to Purkinje cell dystopia and greatly reduced dendritic trees.

4.1. Reduced Purkinje cell dendritic tree size in S361G-PKCγ mice

We have analyzed Purkinje cell morphology in S361G-PKCγ and control mice using rapid Golgi staining. While this method stains many cells in the cerebellar cortex the number of visualized Purkinje cells is rather limited (see for example Fig. 1B). For the quantification we used all stained Purkinje cell present in the sample, but this yielded only a low sampling rate of 15–30 Purkinje cells per cerebellum. Rapid Golgi staining is known to be a delicate method and certainly has its limitations for assessing Purkinje cell dendritic morphology. It cannot be completely excluded that the low sampling rate did bias our quantitative findings, for example if smaller Purkinje cells were more prone to become impregnated by the rapid Golgi procedure. Nevertheless, the size difference of the Purkinje cell dendritic tree from wild type and S361G-PKCγ transgenic mice was very evident. In the wild type cerebellum, the dendritic tree of many Purkinje cells covered the entire thickness of the molecular layer (see Fig. 1G). In the S361G-PKCγ cerebellum, the Purkinje cell dendritic trees hardly reached the top of the molecular layer which still had a normal thickness. In immunostainings with Purkinje cell-specific markers, there was positive staining

throughout the molecular layer, including the distal part (e.g. Fig. 4A) indicating that some Purkinje cells must span the entire molecular layer. The presence of the small Purkinje cells seen in the Golgi study indicates that in the S361G-PKCγ mice the dendritic tree size of many Purkinje cells is reduced. This was not obvious in calbindin or PKCγ stainings (Ji et al., 2014) and demonstrates that these immunostainings do not easily detect reductions of dendritic tree size when they affect only a fraction of Purkinje cells. Due to the extensive overlap of Purkinje cell dendritic trees smaller dendritic trees may be masked by the larger dendritic trees from neighboring cells.

In another study looking at the size of the Purkinje cell dendritic tree using Golgi staining in *hotfoot* mutant mice, a reduction of dendritic tree size was found in the absence of major changes in calbindin staining and molecular layer thickness (Zanjani et al., 2016) confirming the higher sensitivity of Golgi staining compared to immunohistochemical evaluation. In a number of additional mutant mouse models, a reduction of Purkinje cell dendritic tree size has been demonstrated using rapid Golgi staining. These include mouse models of Dyt1 dystonia (Zhang et al., 2011; Song et al., 2014) and a knockout mouse of the matrix metalloproteinase MMP-3 (van Hove et al., 2012). Furthermore, in human specimens from patients with essential tremor a marked reduction of Purkinje cell dendritic tree size was demonstrated (Louis et al., 2014). Taken together these data indicate that a reduction of the Purkinje cell dendritic tree size as revealed by rapid Golgi staining is a sensitive parameter indicating Purkinje cell dysfunction. Our data provide clear evidence for such a reduction of Purkinje cell dendritic tree size in the S361G-PKCγ mouse model of SCA14.

4.2. Subtle changes of climbing fiber innervation in the cerebellum of S361G-PKCγ mice, but severe disorganization in lobule 7

Despite these changes in Purkinje cell dendritic tree size the S361G-PKCγ mice only have a mild ataxic phenotype (Ji et al., 2014) indicating that the cerebellar cortex is essentially functional. This is reflected in the rather normal pattern of climbing fiber innervation as visualized by vGlut2 immunostaining. Climbing fibers target the dendritic tree of Purkinje cells covering approx. 80% of the molecular layer thickness both in WT and S361G-PKCγ mice (Fig. 3I, M). The developmental timing of climbing fiber innervation was similar in WT and S361G-PKCγ mice with climbing fibers being present in the inner part of the molecular layer by P14 (Fig. 3G, K) and extending to the outer part by P28 (Fig. 3H, L). The inferior olivary nucleus, the origin of the climbing fiber projection, appeared normal in cresyl violet stained sections and no major atrophy was apparent (data not shown). This finding is in agreement with the normal climbing fiber innervation of most parts of the cerebellum.

This rather normal pattern of climbing fiber innervation with only minor abnormalities contrasts with the greatly abnormal pattern found around lobule 7. As reported earlier (Ji et al., 2014), in this cerebellar lobule Purkinje cell morphology becomes disrupted and the molecular layer is disorganized. Climbing fiber innervation was strongly reduced and only covered the soma and parts of the primary dendrite of the Purkinje cells (arrows in Fig. 4K, L), in some Purkinje cells it was completely absent. This disorganization of the molecular layer indicates that this cerebellar lobule is probably dysfunctional in S361G-PKCγ mice. Reduced climbing fiber innervation is a hallmark of dysfunction of the cerebellar cortex. In a mouse model of SCA-1 lacking neurodegeneration but showing a distinct behavioral phenotype, reduced climbing fiber innervation was one of the major pathological hallmarks of the disease (Duvick et al., 2010). A similar situation exists for mice deficient for Car8 where the absence of Purkinje cell degeneration contrasts with a marked behavioral phenotype (Jiao et al., 2005; White et al., 2016). These mice also have a reduction in climbing fiber innervation (Miterko and Sillitoe, 2018). Both mouse models share some similarities to the S361G-PKCγ mice because they show an ataxic behavioral phenotype in the absence of Purkinje cell degeneration. The major reduction of climbing fiber innervation in lobule 7 of the S361G-PKCγ mice shows that strong transgene expression does induce a disorganization of the cerebellar cortex and interferes with climbing fiber innervation. The rather subtle changes in the rest of the cerebellar cortex indicate that despite the reduction of dendritic tree size the Purkinje cells there probably function rather normally, as reflected in the rather mild behavioral phenotype of the S361G-PKCγ mice.

4.3. Near normal expression of activity and plasticity markers in the cerebellum of S361G-PKCγ mice, but severe disorganization in lobule 7

We have used three different markers of activity and plasticity to monitor changes in Purkinje cells of S361G-PKCγ mice. With the anti-pS6 staining the activity of the mTORC1 signaling pathway is monitored. This staining is absent in Purkinje cells deficient for RPTOR which have inactive mTORC1 signaling (Angliker et al., 2015) and is increased in Tsc1 mutant mice with increased mTORC1 activity (Tsai et al., 2012). The mTORC1 pathway is essential for cell growth and a wide variety of cellular functions and normally all Purkinje cells are pS6 positive, and this was also the case in most parts of the cerebellum of S361G-PKCγ mice. The virtual absence of pS6 staining in morphologically altered and dystopic Purkinje cells in lobule 7 of S361G-PKCγ mice indicates that these cells are severely compromised in their function and are unlikely to be part of the functional network of the cerebellar cortex. For the activity related gene c-Fos the situation was very similar. In most parts of the cerebellum of the S361G-PKCγ mice there was the typical expression pattern with Purkinje cells having a stronger or weaker c-Fos expression, but all Purkinje cells expressed some c-Fos protein. In lobule 7 where abnormalities in S361G-PKCγ mice are most evident, many Purkinje cells were present with abnormal dendritic morphology and often a dystopic location in the molecular layer. Most of these cells were negative for c-Fos indicating a reduced level of activity. However, some of these cells were also c-Fos positive (Fig. 6D–F). It is not clear whether the c-Fos activation in these cells reflects compensatory mechanisms aiming at a normalization of cellular functions or whether it reflects the activation of pathways which eventually could result in the elimination of these cells. This would be supported by the observation that dystopic Purkinje cells in lobule 7 are more common in young animals compared to older animals (Ji et al., 2014). The expression of the activity marker Arc was rather similar to that of c-Fos. The very similar picture of the activation of c-Fos and Arc confirms an earlier report in which a similar activation has been found after eyeblink conditioning (Kim and Thompson, 2011).

4.4. Expression of mutated S361G-PKCγ and Purkinje cell morphology and function

The results from the Golgi staining show that there is a widespread reduction of Purkinje cell dendritic tree size throughout the cerebellar cortex in S361G-PKCγ mice. This corresponds with the L7-driven widespread expression of the mutated PKCγ gene and the finding that in organotypic slice cultures there is a reduction of Purkinje cell dendritic tree size in most Purkinje cells. It also corresponds to the known negative effect of PKC activity on Purkinje cell dendritic development (Kapfhammer, 2004). In contrast to the reduction seen in Golgi staining, in most parts of the S361G-PKCγ cerebellum immunostainings for Purkinje cell and synaptic markers are normal (Ji et al., 2014). This was confirmed in this study which showed that in most parts of the cerebellum climbing fiber innervation appeared to be intact and by the normal expression of the three different activity and plasticity markers pS6, cFos and Arc. These findings suggest that in most part of the cerebellar cortex the marked reduction of Purkinje cell dendritic tree size is compatible with normal synaptic connections and function showing a substantial potential for functional compensation. Such compensatory mechanisms are well known from neurodegenerative diseases (Gregory et al., 2017) and appear to be in operation also on the level of the cerebellar cortex and are most likely responsible for the rather subtle behavioral phenotype of the S361G-PKCγ mouse model. Such mechanisms might include increased expression of heat shock

proteins (Nakazono et al. 2018), the reduction of ER-stress (Guo et al., 2018) or activation of potassium channels (Bushart et al., 2018). In contrast, in lobule 7 and adjacent parts of lobule 6 there is a much stronger morphological phenotype. In these areas, many Purkinje cells show strong transgene expression and have very small condensed dendritic trees. The cell somata often have a dystopic location in the molecular layer. Furthermore, there is a major reduction of climbing fiber innervation and reduced or absent expression of the activity and plasticity markers. The area around lobule 7 thus appeared to be dysfunctional. In the affected Purkinje cells transgene expression was strong, so the strong phenotype could be partly explained by a strong expression of the L7 promoter in this region around birth and the early postnatal period (Ozol et al., 1999). Less efficient compensatory mechanisms in this region might also contribute to the stronger phenotype. An important contribution of compensatory mechanisms is suggested by the finding that Purkinje cell dendritic development is strongly impaired in cerebellar slice cultures derived from S361G transgenic mice (Ji et al., 2014). Obviously, compensatory mechanisms are expected to be less effective in slice cultures which impose a certain stress on the cerebellar tissue. Our Golgi study demonstrates that throughout the cerebellar cortex, transgene expression is sufficient to affect dendritic tree size of Purkinje cells. Our immunohistochemical findings show, in contrast, that this mild alteration of Purkinje cell dendrites is still compatible with a functional cerebellar cortex. The rather mild phenotype and the effectiveness of the compensatory mechanisms in the S361G-PKCγ transgenic mice is certainly helped by the fact that two normal alleles of PKCγ are still present in addition to the mutated transgene and that transgene expression from the L7 promoter is rather moderate (Ji et al., 2014). It is thus likely that both factors, an early and increased transgene expression and less effective compensatory mechanisms contribute to the strong phenotype in lobule 7.

In conclusion, our findings suggest that the expression of the mutated S361G-PKCγ protein interferes with Purkinje cell development and function resulting in a general reduction of Purkinje cell dendritic tree size, but that the functional deficits can be compensated for in most parts of the cerebellar cortex. A strong morphological phenotype probably associated with severe dysfunction of the cerebellar cortex only develops in the presence of strong transgene expression and less effective compensatory mechanisms in and around lobule 7 in this mouse model.

Acknowledgments

We thank Markus Saxer for technical assistance.

Funding

This work was supported by the Swiss National Science Foundation [grant number 31003A-160038].

References

Angliker, N., Burri, M., Zaichuk, M., Fritschy, J.M., Rüegg, M.A., 2015. mTORC1 and mTORC2 have largely distinct functions in Purkinje cells. Eur. J. Neurosci. 42, 2595–2612.

Armengol, J.A., Sotelo, C., 1991. Early dendritic development of Purkinje cells in the rat cerebellum. A light and electron microscopic study using axonal tracing in 'in vitro' slices. Dev. Brain Res. 64, 95–114.

Bushart, D.D., Murphy, G.G., Shakkottai, V.G., 2016. Precision medicine in spinocerebellar ataxias: treatment based on common mechanisms of disease. Ann. Transl. Med. 4 (2), 25.

Bushart, D.D., Chopra, R., Singh, V., Murphy, G.G., Wulff, H., Shakkottai, V.G., 2018. Targeting potassium channels to treat cerebellar ataxia. Ann. Clin. Transl. Neurol. 5, 297–314.

Chopra, R., Wasserman, A.H., Pulst, S.M., De Zeeuw, C.I., Shakkottai, V.G., 2018. Protein kinase C activity is a protective modifier of Purkinje neuron degeneration in cerebellar ataxia. Hum. Mol. Genet. 27, 1396–1410.

Duvick, L., Barnes, J., Ebner, B., Agrawal, S., Andresen, M., Lim, J., Giesler, G.J., Zoghbi, H.Y., Orr, H.T., 2010. SCA1-like disease in mice expressing wild-type ataxin-1 with a serine to aspartic acid replacement at residue 776. Neuron 67, 929–935.

Gregory, S., Long, J.D., Klöppel, S., Razi, A., Scheller, E., Minkova, L., Papoutsi, M., Mills, J.A., Durr, A., Leavitt, B.R., Roos, R.A.C., Stout, J.C., Scahill, R.I., Langbehn, D.R., Tabrizi, S.J., Rees, G., 2017. Operationalizing compensation over time in neurodegenerative disease. Brain 140, 1158–1165.

Gugger, O.S., Hartmann, J., Birnbaumer, L., Kapfhammer, J.P., 2012. P/Q-type and T-type calcium channels, but not type 3 transient receptor potential cation channels, are involved in inhibition of dendritic growth after chronic metabotropic glutamate receptor type 1 and protein kinase C activation in cerebellar Purkinje cells. Eur. J. Neurosci. 35, 20–33.

Guo, J., Cui, Y., Liu, Q., Yang, Y., Li, Y., Weng, L., Tang, B., Jin, P., Li, X.J., Yang, S., Li, S., 2018. Piperine ameliorates SCA17 neuropathology by reducing ER stress. Mol. Neurodegener. 13, 4.

Hioki, H., Fujiyama, F., Taki, K., Tomioka, R., Furuta, T., Tamamaki, N., Kaneko, T., 2003. Differential distribution of vesicular glutamate transporters in the rat cerebellar cortex. Neuroscience 117, 1–6.

van Hove, I., Verslegers, M., Buyens, T., Delorme, N., Lemmens, K., Stroobants, S., Gantois, I., D'Hooge, R., Moons, L., 2012. An aberrant cerebellar development in mice lacking matrix metalloproteinase-3. Mol. Neurobiol. 45, 17–29.

Ji, J., Hassler, M.L., Shimobayashi, E., Paka, N., Streit, R., Kapfhammer, J.P., 2014. Increased protein kinase C gamma activity induces Purkinje cell pathology in a mouse model of spinocerebellar ataxia 14. Neurobiol. Dis. 70, 1–11.

Jiao, Y., Yan, J., Zhao, Y., Donahue, L.R., Beamer, W.G., Li, X., Roe, B.A., Ledoux, M.S., Gu, W., 2005. Carbonic anhydrase- related protein VIII deficiency is associated with a distinctive lifelong gait disorder in waddles mice. Genetics 171, 1239–1246.

Kapfhammer, J.P., 2004. Cellular and molecular control of dendritic growth and development of cerebellar Purkinje cells. Prog. Histochem. Cytochem. 39, 131–182.

Kim, S., Thompson, R.F., 2011. C-Fos, Arc, and stargazin expression in rat eyeblink conditioning. Behav. Neurosci. 125, 117–123.

Louis, E.D., Lee, M., Babij, R., Ma, K., Cortés, E., Vonsattel, J.P., Faust, P.L., 2014. Reduced Purkinje cell dendritic arborization and loss of dendritic spines in essential tremor. Brain 137, 3142–3148.

Metzger, F., Kapfhammer, J.P., 2000. Protein kinase C activity modulates dendritic differentiation of rat Purkinje cells in cerebellar slice cultures. Eur. J. Neurosci. 12, 1993–2005.

Miterko, L.N., Sillitoe, R.V., 2018. Climbing fiber development is impaired in postnatal Car8 wdl mice. Cerebellum 17, 56–61.

Miyazaki, T., Fukaya, M., Shimizu, H., Watanabe, M., 2003. Subtype switching of vesicular glutamate transporters at parallel fiber-Purkinje cell synapses in developing mouse cerebellum. Eur. J. Neurosci. 17, 2563–2572.

Nakazono, A., Adachi, N., Takahashi, H., Seki, T., Hamada, D., Ueyama, T., Sakai, N., Saito, N., 2018. Pharmacological induction of heat shock proteins ameliorates toxicity of mutant PKCγ in spinocerebellar ataxia type 14. J. Biol. Chem. 293, 14758–14774.

Ozol, K., Hayden, J.M., Oberdick, J., Hawkes, R., 1999. Transverse zones in the vermis of the mouse cerebellum. J. Comp. Neurol. 412, 95–111.

Pandolfo, M., van de Warrenburg, B.P., 2005. Spinocerebellar ataxia type 14: opening a new door in dominant ataxia research? Neurology 64, 1113–1114.

Paulson, H.L., Shakkottai, V.G., Clark, H.B., Orr, H.T., 2017. Polyglutamine spinocerebellar ataxias - from genes to potential treatments. Nat. Rev. Neurosci. 18, 613–626.

Sagar, S.M1., Sharp, F.R., Curran, T., 1988. Expression of c-fos protein in brain: metabolic mapping at the cellular level. Science 240, 1328–1331.

Sherkhane, P., Kapfhammer, J.P., 2017. Chronic pharmacological blockade of the Na+/Ca2+ exchanger modulates the growth and development of the Purkinje cell dendritic arbor in mouse cerebellar slice cultures. Eur. J. Neurosci. 46, 2108–2120.

Shimobayashi, E., Kapfhammer, J.P., 2017. Increased biological activity of protein Kinase C gamma is not required in Spinocerebellar ataxia 14. Mol. Brain 10 (34).

Shimobayashi, E., Kapfhammer, J.P., 2018. Calcium signaling, PKC Gamma, IP3R1 and CAR8 link spinocerebellar ataxias and purkinje cell dendritic development. Curr. Neuropharmacol. 16, 151–159.

Shimobayashi, E., Wagner, W., Kapfhammer, J.P., 2016. Carbonic anhydrase 8 expression in Purkinje cells is controlled by PKCγ activity and regulates Purkinje cell dendritic growth. Mol. Neurobiol. 53, 5149–5160.

Song, C.H., Bernhard, D., Hess, E.J., Jinnah, H.A., 2014. Subtle microstructural changes of the cerebellum in a knock-in mouse model of DYT1 dystonia. Neurobiol. Dis. 62, 372–380.

Soong, B.W., Paulson, H.L., 2007. Spinocerebellar ataxias: an update. Curr. Opin. Neurol. 20, 438–446.

Steward, O., Worley, P.F., 2001. Selective targeting of newly synthesized Arc mRNA to active synapses requires NMDA receptor activation. Neuron 30, 227–240.

Tsai, P.T., Hull, C., Chu, Y., Greene-Colozzi, E., Sadowski, A.R., Leech, J.M., Steinberg, J., Crawley, J.N., Regehr, W.G., Sahin, M., 2012. Autistic-like behaviour and cerebellar dysfunction in Purkinje cell Tsc1 mutant mice. Nature 488, 647–651.

White, J.J., Arancillo, M., King, A., Lin, T., Miterko, L.N., Gebre, S.A., Sillitoe, R.V., 2016. Pathogenesis of severe ataxia and tremor without the typical signs of neurodegeneration. Neurobiol. Dis. 86, 86–98.

Wong, M.M.K., Hoekstra, S.D., Vowles, J., Watson, L.M., Fuller, G., Németh, A.H., Cowley, S.A., Ansorge, O., Talbot, K., Becker, E.B.E., 2018. Neurodegeneration in SCA14 is associated with increased PKCγ kinase activity, mislocalization and aggregation. Acta Neuropathol. Commun. 6, 99.

Wullschleger, S., Loewith, R., Hall, M.N., 2006. TOR signaling in growth and metabolism. Cell 124, 471–484.

Zanjani, H.S., Vogel, M.W., Mariani, J., 2016. Deletion of the GluRδ2 receptor in the hotfoot mouse mutant causes granule cell loss, delayed Purkinje cell death, and reductions in Purkinje cell dendritic tree area. Cerebellum 15, 755–766.

Zhang, L., Yokoi, F., Jin, Y.H., Deandrade, M.P., Hashimoto, K., Standaert, D.G., Li, Y., 2011. Altered dendritic morphology of Purkinje cells in Dyt1 ΔGAG knock-in and Purkinje cell-specific Dyt1 conditional knockout mice. PLoS One 6 (3), e18357.